Lab on a Chip

PAPER

View Article Online
View Journal | View Issue

Electronic control of platelet adhesion using conducting polymer microarrays

Cite this: *Lab Chip*, 2014, **14**, 3043

Lars Faxälv,†*[a] Maria H. Bolin,†[b] Edwin W. H. Jager,[bc] Tomas L. Lindahl[a] and Magnus Berggren[b]

Received 14th February 2014,
Accepted 29th May 2014

DOI: 10.1039/c4lc00201f

www.rsc.org/loc

We hereby report a method to fabricate addressable micropatterns of e-surfaces based on the conducting polymer poly(3,4-ethylenedioxythiophene) doped with the anion tosylate (PEDOT:Tos) to gain dynamic control over the spatial distribution of platelets *in vitro*. With thin film processing and microfabrication techniques, patterns down to 10 μm were produced to enable active regulation of platelet adhesion at high spatial resolution. Upon electronic addressing, both reduced and oxidized surfaces were created within the same device. This surface modulation dictates the conformation and/or orientation, rather than the concentration, of surface proteins, thus indirectly regulating the adhesion of platelets. The reduced electrode supported platelet adhesion, whereas the oxidized counterpart inhibited adhesion. PEDOT:Tos electrode fabrication is compatible with most of the classical patterning techniques used in printing as well as in the electronics industry. The first types of tools promise ultra-low-cost production of low-resolution (>30 μm) electrode patterns that may combine with traditional substrates and dishes used in a classical analysis setup. Platelets play a pronounced role in cardiovascular diseases and have become an important drug target in order to prevent thrombosis. This clinical path has in turn generated a need for platelet function tests to monitor and assess platelet drug efficacy. The spatial control of platelet adherence presented here could prove valuable for blood cell separation or biosensor microarrays, *e.g.* in diagnostic applications where platelet function is evaluated.

1. Introduction

Patterning of various chemical or biological functionalities on a single surface has become a very attractive route to compress a vast array of test variables into a single experiment. The use of patterns for multiplex detection and quantification purposes has predominantly been applied to molecules, but there is also a growing interest in applying these techniques to cell studies where different cell types or different cell functions can be assessed simultaneously on the same surface.[1–4] One such area of interest is clinical tests of blood in order to identify a variety of physiological conditions or to monitor the effectiveness of treatments. A specific category of such tests focuses on platelets, blood cells which are involved in the important wound sealing process that stops bleeding after a blood vessel injury. Platelets also play a pronounced role in cardiovascular diseases and have become an important drug target in order to prevent thrombosis.[5] This clinical path has in turn generated a need for platelet function tests to monitor and assess platelet drug efficacy.[6] In this context, it is desired to develop a system where the platelet adhesion conditions could be controlled in a spatio-temporal adjustable manner, for instance, by fabricating micropatterned systems or microarrays to create a controllable environment of cues presented to the platelets.

Platelets are non-nucleated cells and represent one of the main components in the hemostatic (blood stopping) system. Upon vascular trauma they rapidly adhere to a damaged vessel wall to form a cellular plug that initially stops bleeding. To form the required multilayer cellular plug, platelets adhere to each other by binding soluble fibrinogen to the activated GPIIb-IIIa receptor (integrin αIIbβ3) in a process termed platelet aggregation. Therefore, this ligand binding is a fundamental step for the hemostatic function but has also proved to be a central mechanism in blood interactions with biomaterials, in which surface adsorbed fibrinogen is a key regulator of platelet adhesion to blood-contacting biomaterials.[7]

Organic electronic materials have proven to be unique in many senses to regulate and record various processes of biological systems even down to the individual cell level.[8]

[a] *Clinical Chemistry, Dept. of Clinical and Experimental Medicine, Linköping University, SE-581 85 Linköping, Sweden. E-mail: lars.faxalv@liu.se*
[b] *Organic Electronics, Dept. of Science and Technology, Linköping University, SE-601 74 Norrköping, Sweden*
[c] *Biosensors & Bioelectronics Centre, Dept. of Physics, Chemistry and Biology, Linköping University, SE-581 83 Linköping, Sweden*
† Equal contributions.

Organic electronic materials can combine ionic with electronic conductivity and the materials can also exhibit electrochemical and electronic activities. The materials can also function and operate in the hydrated state and are typically soft and flexible.[9,10] Together, these features make organic electronic materials excellent systems to define a desired chemical-to-electronic and electronic-to-chemical signal translation that can be explored in various sensor and actuator devices, respectively, *in vitro* and *in vivo*. Various organic field effect and electrochemical transistors, drug delivery components, electrodes and electrochemical surface (e-surface) switches have been explored in the past to define a bridge between technology and biology for various therapy, biotechnology and medical applications.[11] In particular, the e-surfaces have been explored as controllable surfaces and scaffolds for the cultivation of cells.[12,13] As the e-surface is switched in between different electrochemical states, the conformation and activity of extracellular matrix proteins, growth factors, *etc.* may be modulated, thus controlling the fate of the cell system.

In this work, we report a method to fabricate addressable micropatterns of e-surfaces based on the conducting polymer poly(3,4-ethylenedioxythiophene) doped with the anion tosylate (PEDOT:Tos) to gain dynamic control over the spatial distribution of platelets *in vitro*. Utilizing thin film processing and microfabrication techniques, desired patterns down to 10 μm were achieved to enable active regulation of platelet adhesion at high spatial resolution. Upon electronic addressing, both reduced and oxidized surfaces were created within the same device. The changes in the electrochemical state of PEDOT:Tos result in a reversible modification of the surface properties of the material.[13] This surface modulation dictates the conformation and/or orientation, rather than the concentration, of surface proteins, thus indirectly regulating the adhesion of platelets.

2. Materials and methods

2.1 Fabrication of gold electrodes on PET substrates

Polyethylene terephthalate (PET) foil was used as the substrate. Its surface was cleaned with acetone, dried in an oven (110 °C) and then pretreated with O_2 plasma. The PET surface was then coated with a gold film (70 nm) together with an adhesion layer of titanium (10 nm). Both metal layers were deposited by thermal evaporation. Shipley 1813 photoresist was then deposited onto the gold surface after a pretreatment step with O_2 plasma. The photoresist was baked at 110 °C for 90 seconds. The layer of gold was patterned using standard UV photolithography and wet chemically etched using an I_2 + KI etch. The exposed titanium was removed using a SF_6 plasma etch step. Finally, the remaining photoresist was removed with acetone.

2.2 Polymer deposition

Polyethylene terephthalate (PET) substrates, with and without patterned gold electrodes (see 2.1), were cleaned with acetone and dried in an oven at 110 °C prior to deposition. Solutions of 3,4-ethylenedioxythiophene (EDOT, Sigma-Aldrich), 20% iron(III) tris-*p*-toluenesulfonate (iron tosylate (Tos), Baytron C, H. C. Stark GmbH) and pyridine (Sigma-Aldrich), mixed in butanol, were bar-coated onto the substrates.[13] The wet films were heated on a hotplate at 60 °C to facilitate chemical polymerization and to evaporate non-reacted residues. The remaining iron tosylate was removed by sequential washing with butanol, isopropanol, and DI water. The resulting PEDOT:Tos-coated substrates were cleaned with acetone and deionized water and finally dried in an oven at 110 °C before further processing. The same coating procedure was accomplished with Zeonor 1060R substrates (a generous gift from Åmic AB, Uppsala, Sweden). Two neighboring electrodes were defined on the coated surfaces by disrupting the conductive film simply with a sharp blade along the center of the surface. Successful electrode separation was verified by electrical resistance measurements.

2.3 Fabrication of electroactive micropatterns

A protecting layer of polyvinylidene difluoride (PVDF) polymer (Solvay) was spin casted and baked at 110 °C on top of the PEDOT:Tos layer (as described in 2.2) before the Shipley 1805 photoresist was deposited and patterned using standard photolithography. The layer that was not covered by the photoresist was removed using an O_2/CF_4 plasma etch step. Chemically over-oxidized patterns of the PEDOT:Tos film were defined by exposing the non-covered PEDOT:Tos areas to sodium hypochlorite solution (NaOCl, 1% vol./vol., 1 min).[14] The resist and the remaining PVDF protecting layer were then removed using an acetone bath and the substrates were rinsed with DI water. In some structures, a layer of SU-8 2010 (MicroChem) was patterned by standard photolithography on top of the over-oxidized PEDOT micropatterns.

2.4 Active cell culture dish

Functional dishes were created by fitting a polydimethylsiloxane (PDMS) gasket with defined wells on top of the two-electrode or micropatterned substrates (see 2.2 and 2.3). A schematically illustrated cross-section of the two-electrode configuration is presented in Fig. 1. The two-electrode configuration utilized three juxtaposed PDMS wells mounted in such a way that both electrodes were exposed in each well, giving a triplicate of the e-surface electrode configuration on each substrate.

2.5 Fibrinogen adsorption

Using phosphate-buffered saline (PBS) as an electrolyte, the electrodes were electrochemically switched by applying a potential of 1.0 V between two electrodes. Next, the wells were washed thoroughly with PBS in the switched state. PBS containing 0.1, 1 or 10 mg mL^{-1} AlexaFluor 488 fibrinogen (Invitrogen) was added to the wells and thereafter incubated for 120 minutes with applied electric potential. To investigate the conformational state of adsorbed fibrinogen, two-electrode

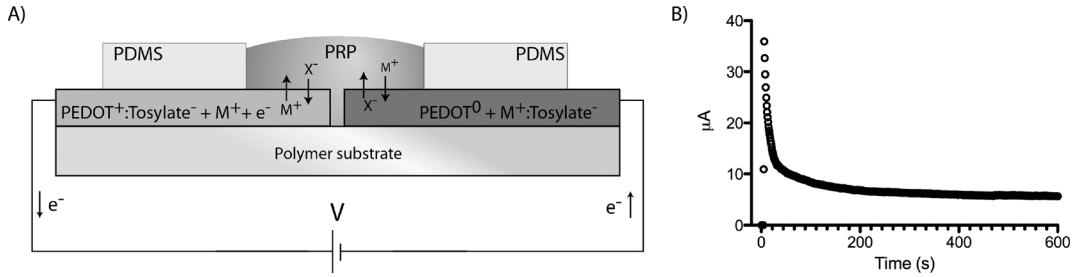

Fig. 1 A) Schematic illustration of the patterned cell culture dish showing two PEDOT electrodes. A positive potential is applied to the left electrode (anode) which is then oxidized, and a negative potential is applied to the right electrode (cathode), reducing it to the neutral state. This redox process is accompanied by an ion flow into/out of the polymer matrix as illustrated by an arbitrary cation M^+ and anion X^-. A PDMS layer comprising wells is placed on the patterned surface, thus forming a functional device that can contain the platelet-rich plasma (PRP). B) Current *versus* time graph of reduction/oxidation of PEDOT electrodes after applying a 1.0 V potential with platelet-rich plasma as the electrolyte.

configuration wells were incubated for 30 minutes in platelet-free plasma, and after washing incubated with 1 μg mL^{-1} FITC conjugated polyclonal anti-fibrinogen (Diapensia HB, Linköping, Sweden) or 1 μg mL^{-1} monoclonal anti-fibrinogen (clone 9F9, BioCytex, Marseille, France) in PBS for 20 minutes. The latter antibody, clone 9F9, has a high affinity for fibrinogen in the conformation state when bound to platelets or plastic surfaces but not to the conformational state of fibrinogen in solution.[15] For analysis, the wells were washed with PBS and fluorescence images of the surfaces were captured with fixed exposure time using a Zeiss Axio Observer Z1 fluorescence microscope fitted with an Axiocam MRm camera. Measurements of the fluorescence images were performed using the software ImageJ (NIH).

2.6 Platelet adhesion

Blood was drawn from healthy volunteers and collected in 6 mL BD Vacutainer heparin tubes (BD Diagnostics). Platelet-rich plasma was prepared by centrifuging filled tubes at 180 *g* for 20 minutes and collecting the supernatant. The PEDOT:Tos coated surfaces were either preadsorbed with 1 mg mL^{-1} fibrinogen or 1 mg mL^{-1} von Willebrand factor in PBS or used directly. All PEDOT:Tos surfaces were however washed in PBS in the switched state before exposure to the platelets. Platelet adhesion was allowed to take place by adding platelet-rich plasma on the top of the surface followed by incubation for 30 minutes with a constant potential of 1.0 V. To evaluate platelet adhesion response to applied electrode voltage, platelet-rich plasma was incubated for 10 minutes on the PEDOT surface with electrode potentials ranging from 0.5 to 2.0 V. The surfaces were thereafter thoroughly rinsed and adhered platelets were detected by following either of two routes: (i) surfaces were kept in PBS after rinsing and platelets were studied under the microscope using phase contrast, or (ii) platelets were fixed with 3.7% *para*-formaldehyde (PFA) (Sigma-Aldrich) in PBS for 15 minutes, permeabilized with 0.1% Tritron X-100 (Sigma-Aldrich) in PBS for 3 minutes, and thereafter labeled with AlexaFluor 546-phalloidin for 20 minutes. Surfaces were thereafter rinsed with PBS and water, dried in flowing air and studied by fluorescence microscopy. Transmitted light, phase contrast and fluorescence images were captured using a Zeiss Axio Observer Z1. To quantify fluorescent labeled platelets, the particle analyzer function in ImageJ (NIH) was used.

3. Results and discussion

3.1 Characterization of micropatterns of electroactive surfaces

Addressable micropatterns of gold and thin film PEDOT:Tos coated on PET foil were fabricated (Fig. 2A). The thermally evaporated and patterned thin films of titanium and gold (10 nm and 70 nm in thickness, respectively) showed good adhesion to the substrates. The PEDOT:Tos solution was bar coated on top of the inert gold electrodes resulting in a homogenous film with a thickness of 150 nm. The chemical over-oxidation with NaOCl divided the conducting film into several electronically (but not ionically) isolated micropatterned electrodes with a lateral size ranging from 10 μm to 1000 μm separated by a distance of 10–1000 μm. By using the over-oxidation method instead of etching, the conductive PEDOT:Tos layer could be patterned into electrically insulated microstructures without introducing a topography step between the electrodes. The devices were designed as microarrays with individually addressable microelectrodes in 3 × 3 and 4 × 4 configuration squares as well as two-electrode interdigitated finger structures. On a subset of devices an insulating layer of SU-8 (10–100 μm thick) was deposited on top of the over-oxidized PEDOT:Tos pattern.

A droplet of 0.1 M NaCl electrolyte was placed on top of the device covering the matrix or fingers but not the contact pads (Fig. 2B). In the presence of the electrolyte the device functions as an electrochemical circuit. In order to characterize the device a potential difference of 1.0 V was applied to individual microelectrodes resulting in an electrochemical switch of the PEDOT:Tos electrodes in the addressed structures. Two addressed electrodes can be regarded as an electrochemical cell where reduction occurs at the negative electrode and oxidation at the positive electrode, based on reaction (1). Since the film of PEDOT:Tos includes immobile anions (Tos), cations M^+ from the electrolyte move in or out

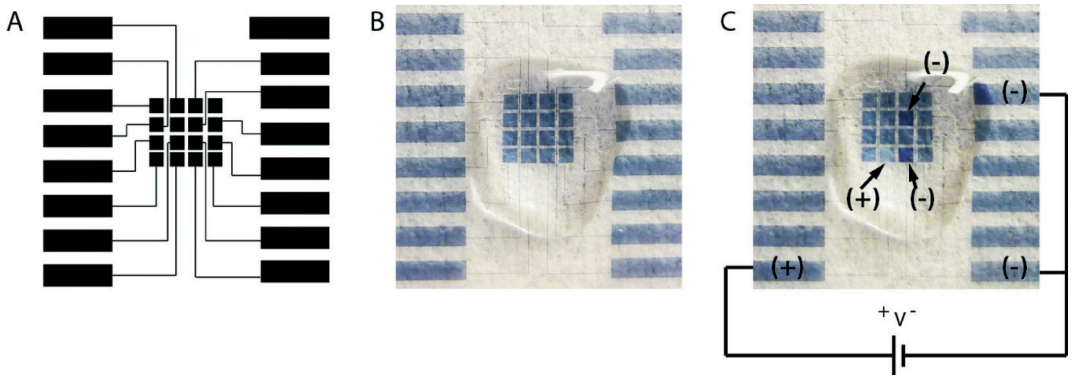

Fig. 2 A) Schematic illustration of addressable micropatterns of PEDOT:Tos surfaces. B) The blue PEDOT:Tos microelectrodes are electronically separated by the transparent chemically over-oxidized patterns of PEDOT:Tos. C) In the presence of an electrolyte the device functions as an electrochemical circuit when a potential is applied to the electrodes. Dark blue corresponds to the reduced state, whereas light blue corresponds to the oxidized state.

of the film during reactions to compensate for the change in electronic charge.

$$\text{PEDOT}^{+}\text{:Tosylate}^{-} + e^{-} + M^{+} \leftrightarrow \text{PEDOT}^{0} + M^{+}\text{:Tosylate}^{-} \quad (1)$$

The electrochromic response of the individual microelectrodes upon the electrochemical switching (Fig. 2C) was monitored. As can be seen, the microelectrodes clearly shift from the light sky-blue semi-oxidized state,[16] through the deep-blue (neutral/reduced) state and to almost completely transparent in the fully oxidized state. The adjacent, non-addressed microelectrodes remain in the as fabricated, semi-oxidized state. This experiment demonstrates individual control of the electrochemical state of the individual microelectrodes.

3.2 Fibrinogen adsorption and platelet adhesion

Fibrinogen adsorption and platelet adhesion were investigated on reduced and oxidized PEDOT:Tos e-surfaces in a standard two-electrode setup (see Fig. 1). The platelet adhesion experiments also included a non-addressed PEDOT:Tos surface as a reference surface. Adsorbed fibrinogen was quantified using a fluorescent labeled fibrinogen. As can be seen in Fig. 3A, it is evident that there is no major difference between reduced and oxidized PEDOT:Tos in terms of fibrinogen adsorption, although a non-significant inclination towards a slightly larger quantity of adsorbed fibrinogen was found on the oxidized electrode. Interestingly, however, a large difference in platelet adhesion was evident when comparing electrodes in the different redox states (Fig. 3B). The reduced electrode induces platelet adhesion to a much greater extent compared to its oxidized counterpart. This was confirmed for both fibrinogen pre-coated electrodes and electrodes exposed directly to the platelet-rich plasma. The non-addressed PEDOT:Tos reference electrode demonstrated a similar behavior to that of the reduced electrode, except from showing slightly less platelet adhesion when the electrode was pre-coated with plasma, indicating that it is primarily the oxidation of the PEDOT electrode that alters the interfacial conditions and thereby regulates platelet adhesion negatively.

It is well known that very small amounts of surface-adsorbed fibrinogen are sufficient to facilitate platelet adhesion,[17] and more recently it has also been shown that it is not primarily the amount of adsorbed fibrinogen that

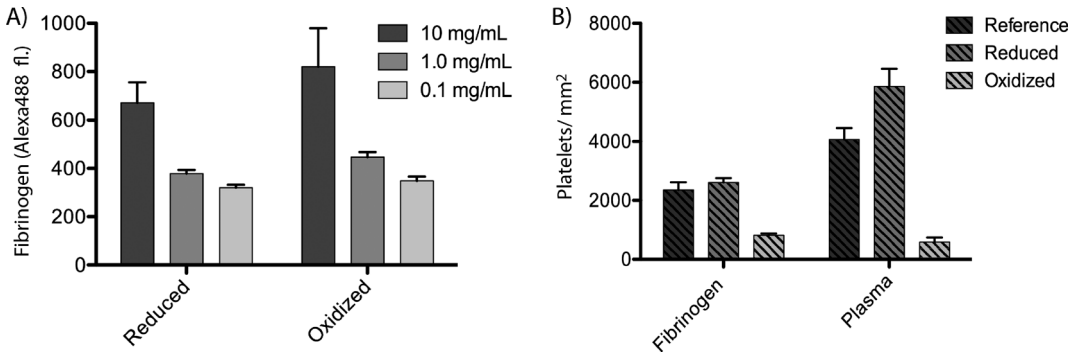

Fig. 3 Fibrinogen adsorption and platelet adhesion to reduced and oxidized PEDOT:Tos coated surfaces. A) Adsorption of fluorescent labeled fibrinogen on the reduced and oxidized electrodes from a solution containing 0.1, 1, or 10 mg mL^{-1} AlexaFluor 546 fibrinogen (n = 4). B) Platelet adhesion to reduced, oxidized and reference electrodes from platelet-rich plasma (n = 3). The electrode surfaces were either pre-coated with 1 mg mL^{-1} fibrinogen (Fibrinogen) in PBS or used directly (Plasma).

dictates the extent of platelet adhesion but rather the conformation of the adsorbed fibrinogen.[18,19] In the light of these previous findings, the conformational state of the adsorbed fibrinogen could most probably be the driving force controlling platelet adhesion in our experiments. Further adding support to fibrinogen conformation-dependent adhesion on these electrodes are previously published findings that the redox state of conducting polymers has induced differential conformation changes in fibronectin,[13,20,21] thereby regulating cell binding and proliferation on similar surfaces. An existing method that could provide further information about this mechanism is circular dichroism (CD), which recently has been adapted to investigate conformational changes of proteins bound to surfaces.[18] To further elucidate a potential mechanism behind the difference in platelet adhesion, we utilized the fibrinogen antibody clone 9F9 produced to recognize the conformational state of fibrinogen when adsorbed on plastic surfaces and not the conformational state when it is in solution.[15] Comparing the binding of clone 9F9 with a polyclonal fibrinogen antibody by forming a ratio of 9F9/polyclonal, the fluorescence intensity demonstrated relatively more 9F9 bound by reduced (0.67 ± 0.08) than by oxidized (0.38 ± 0.10) PEDOT (n = 3). The smaller fraction of fibrinogen recognized by the 9F9 on the oxidized surface indicates that more adsorbed fibrinogen retains a similar conformational state to that of fibrinogen in solution (not recognized by 9F9).[15] As mentioned previously, the natural conformation of soluble fibrinogen under physiological conditions is such that platelets are unable to bind, unless the platelet becomes activated and thereby induces a structural change in the GPIIb-IIIa fibrinogen receptor that enables binding.[22] Platelet adhesion to oxidized and reduced electrodes was also analyzed after pre-incubation with the adhesion protein von Willebrand factor. Although there was an effect on platelet adhesion when comparing reduced with oxidized electrodes, resulting in 1.5 ± 0.3 times more adhesion to reduced than oxidized electrodes, the effect was much more pronounced after incubation with fibrinogen, resulting in 3.3 ± 0.6 times more adhesion (n = 3).

We also performed a platelet adhesion experiment at different reduction/oxidation voltages. As an indication of the reduction/oxidation level we utilized the changes in light absorbance of the electrodes upon application of electric potential, using physiological saline solution as the electrolyte. The gray level ratios between oxidized and reduced electrodes from photographs were calculated and are presented in Fig. 4A, demonstrating the largest differences between 0.5 and 1.0 V. Corresponding platelet adhesion experiments (Fig. 4B) also revealed the largest difference in platelet adhesion between 0.5 and 1.0 where a dramatic decrease in platelet adhesion to the oxidized electrode was evident.

3.3 Platelet adhesion on micropatterned surfaces

Micropatterned PEDOT:Tos surfaces were used to study micro-scale platelet adhesion to electrodes in different redox states (Fig. 5). The microelectrodes were individually addressed, switched to the reduced or oxidized state, or left at open circuit as a reference. The different redox states applied can be seen as an increment or decrement in light absorption of the electrode in the micrograph in Fig. 5A (close-up in Fig. 5D), and further emphasized with an applied pseudo-color in Fig. 5B. The fluorescence micrograph of platelet adhesion to the electrodes presented in Fig. 5C (close-up in Fig. 5E) shows increased platelet adhesion to the reduced electrodes while the almost complete absence of platelet adhesion appeared along the oxidized electrodes. Equivalent amounts of adhesion on both the reference electrodes and the background surface were found, similar to the macro-electrodes (Fig. 3B). The images show that platelet

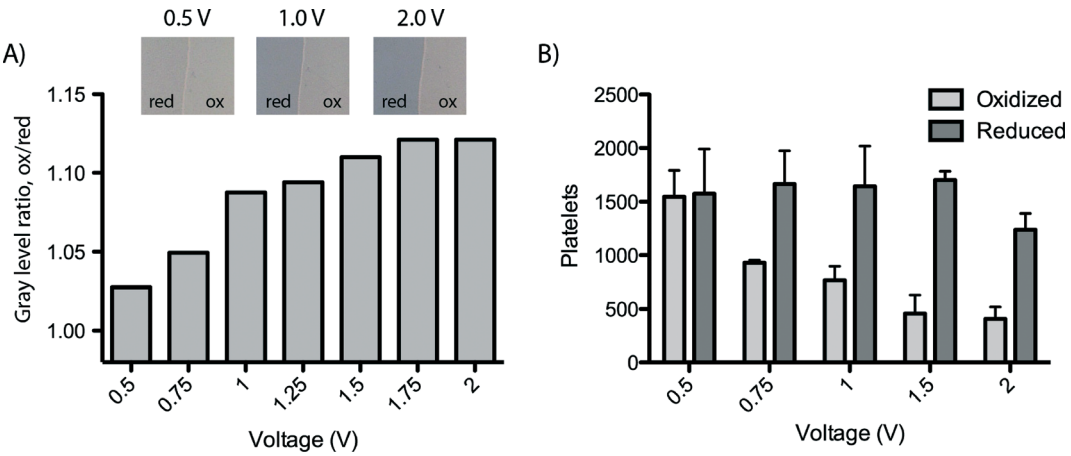

Fig. 4 Platelet adhesion to electrodes in different degrees of reduction/oxidation. A) The degree of reduction/oxidation was evaluated in photographs (shown above the bars) of the two-electrode configuration by their light absorbing properties. The gray level ratios of the oxidized/reduced electrodes are presented. B) Platelet adhesion (platelets mm^{-2}) in the two-electrode configuration measured after 10 minute incubation with platelet-rich plasma at different electric potentials (n = 3).

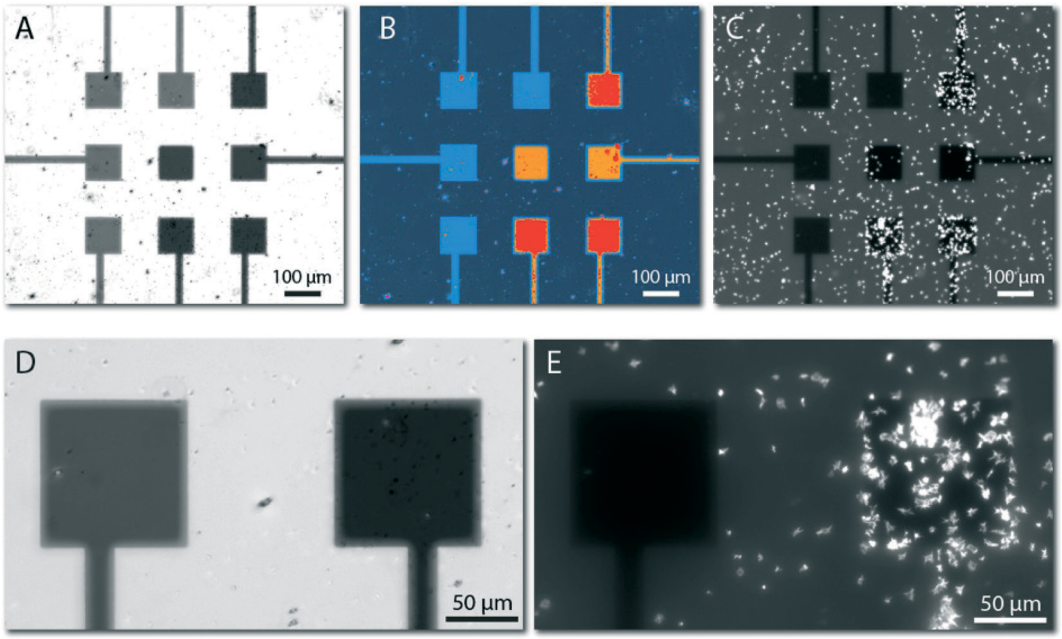

Fig. 5 Platelet adhesion to a micropatterned PEDOT:Tos surface. A) Bright-field image of the patterned, electrically addressed electrodes. The oxidized electrodes have a lighter shade of gray. B) Application of a color map to (A) reveals that the three reduced electrodes are slightly darker (red in the image) compared to the reference (orange) and oxidized (blue) electrodes. C) Fluorescence image of platelets adhered to the addressed electrodes after 30 minutes of exposure to platelet-rich plasma. Platelets are labeled with a fluorescent actin probe (AlexaFluor 546 phalloidin). D) Bright-field and E) fluorescence images of platelet adhesion at a greater magnification of the two lower left electrodes in the previous images (oxidized and reduced electrodes).

adhesion can be regulated with high spatial resolution *via* the applied potential.

In order to achieve more well-defined platelet patterning, it is desired to prevent platelet adhesion to the surrounding substrate. Therefore, we patterned SU-8 in the gap between the electrodes as a platelet repelling layer. As can be seen in Fig. 6 this strategy proved to have functional purposes and no platelets were detected in the gap area covered with SU-8. This additional modification of the patterned electrode surface defines a strategy to confine cell adhesion only to the actual electrodes, which certainly is of great interest for various applications.

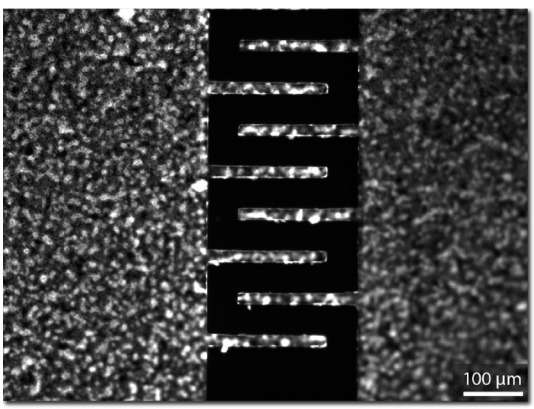

Fig. 6 An SU-8 pattern was used in between electrodes (black meandering path in the figure) as a platelet-repelling layer. It resulted in selective adhesion limited to the electrode material only. The electrodes were not electrically addressed in the image.

4. Conclusions

In the present work we demonstrate precise control of platelet adhesion to individual PEDOT:Tos structures on a micropatterned surface by local electrochemical reduction or oxidation. Reduced electrodes facilitate platelet adhesion whereas the oxidized state of PEDOT:Tos prevents platelets from adhering. The results from fibrinogen adsorption experiments indicate that the difference in platelet adhesion does not originate from the differences in the amount of adsorbed fibrinogen. Considering our own data and with support from earlier studies[18,19] we propose that the conformation of the fibrinogen protein bound to the oxidized PEDOT:Tos is to a large degree in the native state (otherwise found in solution) and that this may regulate the adhesion process negatively, since non-activated platelets are unable to bind fibrinogen in this conformation.

Previous studies have showed that both patterned hydrogel coatings[23] and micro-contact printing[24] can be employed to achieve spatial control of platelet adhesion. However, these routes do not provide dynamic control and are therefore not as flexible as an electroactive surface, an e-surface, where each patterned microelectrode can be addressed individually to obtain specified characteristics within seconds.

Here we present a proof of concept regarding the microfabrication of electroactive PEDOT:Tos. Our switchable

micropatterns or microarrays open up for fundamental studies of cell adhesion behavior and complex manipulation of the adhesion characteristics in a highly parallel manner. High resolution patterns that enable dynamic control, addressed adhesion, and variation in local chemical microenvironments are of extensive interest for numerous fields within the life sciences. Precise control over the surface properties is a powerful tool in regulating the cues for cell growth, for instance, in order to form systems such as tissue and to develop implantable devices. Fabrication of PEDOT:Tos electrodes is compatible with most of the classical patterning techniques used in printing as well as in the electronics industry. The first types of tools promise ultra-low-cost production of low-resolution (>30 μm) electrode patterns that may combine with traditional substrates and dishes used in classical analysis setup. The latter type of tools offers us the possibility to achieve an electrode resolution below 1 μm and thus enables us to electronically control the adhesion characteristics of single platelets.

The spatial control of platelet adherence could be further investigated and potentially proved valuable for blood cell separation or biosensor microarrays, *e.g.* where the hemostatic and thrombotic properties of platelets are evaluated. There are diagnostic instruments on the market for evaluation of platelet function,[25] for example, Multiplate™ from Pentapharm and VerifyNow™ from Accumetrics, but there is still a need for small user-friendly instruments aimed for point-of-care and home use. An additional benefit of using the electroactive patterns, besides the capability of regulating platelet adhesion, is that it may also be possible to simultaneously detect adhesion/aggregation events with *e.g.* impedance measurements, as described previously.[26]

References

1 A. Khademhosseini, R. Langer, J. Borenstein and J. P. Vacanti, *Proc. Natl. Acad. Sci. U. S. A.*, 2006, **103**, 2480–2487.
2 I. Beaulieu, M. Geissler and J. Mauzeroll, *Langmuir*, 2009, **25**, 7169–7176.
3 J. El-Ali, P. K. Sorger and K. F. Jensen, *Nature*, 2006, **442**, 403–411.
4 M. A. Cole, N. H. Voelcker, H. Thissen and H. J. Griesser, *Biomaterials*, 2009, **30**, 1827–1850.
5 L. K. Jennings, *Thromb. Haemostasis*, 2009, **102**, 248–257.
6 A. D. Michelson, *Am. J. Cardiol.*, 2009, **103**, 20A–26A.
7 W. B. Tsai, J. M. Grunkemeier, C. D. McFarland and T. A. Horbett, *J. Biomed. Mater. Res.*, 2002, **60**, 348–359.
8 K. Tybrandt, K. C. Larsson, S. Kurup, D. T. Simon, P. Kjäll, J. Isaksson, M. Sandberg, E. W. H. Jager, A. Richter-Dahlfors and M. Berggren, *Adv. Mater.*, 2009, **21**, 4442–4446.
9 Z. Zhang, R. Roy, F. J. Dugré, D. Tessier and L. H. Dao, *J. Biomed. Mater. Res.*, 2001, **57**, 63–71.
10 P. Åsberg and O. Inganäs, *Biosens. Bioelectron.*, 2003, **19**, 199–207.
11 M. Berggren and A. Richter-Dahlfors, *Adv. Mater.*, 2007, **19**, 3201–3213.
12 C. Saltó, E. Saindon, M. Bolin, A. Kanciurzewska, M. Fahlman, E. W. H. Jager, P. Tengvall, E. Arenas and M. Berggren, *Langmuir*, 2008, **24**, 14133–14138.
13 K. Svennersten, M. H. Bolin, E. W. H. Jager, M. Berggren and A. Richter-Dahlfors, *Biomaterials*, 2009, **30**, 6257–6264.
14 P. Tehrani, N. D. Robinson, T. Kugler, T. Remonen, L. O. Hennerdal, J. Häll, A. Malmström, L. Leenders and M. Berggren, *Smart Mater. Struct.*, 2005, **14**, N21–N25.
15 C. Abrams, N. Ellison, A. Budzynski and S. Shattil, *Blood*, 1990, **75**, 128–138.
16 E. Said, P. Andersson, I. Engquist, X. Crispin and M. Berggren, *Org. Electron.*, 2009, **10**, 1195–1199.
17 W. B. Tsai, J. M. Grunkemeier and T. A. Horbett, *J. Biomed. Mater. Res.*, 1999, **44**, 130–139.
18 B. Sivaraman, K. P. Fears and R. A. Latour, *Langmuir*, 2009, **25**, 3050–3056.
19 B. Sivaraman and R. A. Latour, *Biomaterials*, 2010, **31**, 832–839.
20 A. Kotwal and C. E. Schmidt, *Biomaterials*, 2001, **22**, 1055–1064.
21 P. J. Molino, M. J. Higgins, P. C. Innis, R. M. I. Kapsa and G. G. Wallace, *Langmuir*, 2012, **28**, 8433–8445.
22 B. Savage and Z. M. Ruggeri, *J. Biol. Chem.*, 1991, **266**, 11227–11233.
23 T. Ekblad, L. Faxälv, O. Andersson, N. Wallmark, A. Larsson, T. L. Lindahl and B. Liedberg, *Adv. Funct. Mater.*, 2010, **20**, 2396–2403.
24 L. Basabe-Desmonts, S. Ramstrom, G. Meade, S. O. ÄôNeill, A. Riaz, L. P. Lee, A. J. Ricco and D. Kenny, *Langmuir*, 2010, **26**, 14700–14706.
25 A. D. Michelson, *Circulation*, 2004, **110**, e489–e493.
26 D. C. Cardinal and R. J. Flower, *J. Pharmacol. Methods*, 1980, **3**, 135–158.